# Magnus Effect on a Spinning Satellite in Low Earth Orbit

Sahadeo Ramjatan[1] and Norman Fitz-Coy[2]
*University of Florida, Gainesville, FL  32611*

Alvin Garwai Yew[3]
*NASA GSFC, Greenbelt, MD 20771*

**A spinning body in a flow field generates an aerodynamic lift or Magnus effect that displaces the body in a direction normal to the freestream flow. Earth orbiting satellites with substantial body rotation in appreciable atmospheric densities may generate a Magnus force to perturb orbital dynamics. We investigate the feasibility of using this effect for spacecraft at a perigee of 80km using the Systems Tool Kit (STK). Results show that for a satellite of reasonable properties, the Magnus effect doubles the amount of time in orbit. Orbital decay was greatly mitigated for satellites spinning at 10000 and 15000RPM. This study demonstrates that the Magnus effect has the potential to sustain a spacecraft's orbit at a low perigee altitude and could also serve as an orbital maneuver capability.**

## Nomenclature

| | | |
|---|---|---|
| $\vec{h}$ | = | orbit angular momentum |
| $\vec{V}$ | = | relative velocity |
| $\alpha_\tau$ | = | thermal accommodation coefficient |
| $K_n$ | = | Knudsen number |
| $\vec{r}$ | = | position of the satellite relative to Earth's center |
| $\mu$ | = | standard gravitational parameter |
| $\vec{a_P}$ | = | resultant vector of all the perturbing accelerations |
| $\vec{f}$ | = | perturbing acceleration |
| $a$ | = | semi-major axis |
| $e$ | = | eccentricity |
| $i$ | = | inclination |
| $r$ | = | radius of spherical satellite |
| $\omega$ | = | angular velocity of satellite |
| $\rho$ | = | free-stream density |
| $C_l$ | = | Magnus lift coefficient |
| $C_d$ | = | Drag Coefficient |
| $A$ | = | Reference Area |
| $\mu$ | = | dynamic viscosity |
| $R$ | = | specific gas constant |
| $D$ | = | diameter of sphere |
| $T$ | = | temperature |
| $T$ | = | torque |

## I.  Introduction

There has been the emergence of satellite technology to perform advanced scientific missions including performing in-situ atmospheric research in the low Ionosphere-Thermosphere region. For example, projects including the QB50 Cubesat program will launch cubesats to perform atmospheric research in the lower thermosphere

---

[1] Graduate Student, 231 MAE-A, University of Florida, AIAA Student Member
[2] Associate Professor, Mechanical & Aerospace, 231 MAE-A, University of Florida,  Associate Fellow AIAA
[3] Aerospace Engineer, NASA GSFC, 8800 Greenbelt Rd, MD

1
American Institute of Aeronautics and Astronautics

and to serve as platforms for in-orbit demonstrations (IOD). In Low Earth Orbit (LEO), aerodynamic forces in the form of atmospheric drag perturb orbital trajectories, sometimes in an unpredictable fashion, potentially leading to premature reentry and end-of-life (EOL). However, when satellite surfaces are configured for specific angles of incidence relative to the freestream flow, particularly for sufficiently long durations near the perigee, aerodynamic lift may have an appreciable effect on preserving orbital dynamics [1]. For example, a stabilized disk-shaped satellite may be inclined at the same angle to the air flow at the region of perigee, where aerodynamic forces are greatest for successive revolutions. As a result, the resulting lift would have an appreciable effect on the orbit for perigee heights up to 500km [2]. Furthermore, a spinning body in a fluid creates a nonsymmetrical flow pattern that generates an aerodynamic lift that is commonly described as the Magnus effect. This effect has been the subject of great interest in the history of fluid physics and is named after Professor Gustav Magnus who established that a lifting force is developed by a spinning cylinder placed in an air flow [3]. For example, Newton observed that a transverse force acts on a spinning sphere moving through a fluid and Robins observed a similar effect in the trajectory of cannon balls [4]. A description of the Magnus effect was done by Lord Rayleigh who predicted that the lift was proportional to the speed of rotation and translation. Some of the earliest inventions incorporating this effect included the Flettner rotor which was a sailboat whose sail used a rotating cylinder, which produced a Magnus lift thereby generating a thrust to push the boat forward. Similarly, a popular invention was the Magnus airplane where the Magnus lift was produced by wings made of rotating cylinders. However, the relatively large drag induced by the cylindrical form made the design impractical. Moreover, the Magnus Effect can be seen in many applications including rotary sails, propeller blades, wings, wind turbines, and in the movement of weather systems [4]. For example, in hurricane formation a hurricane will stall over open water spinning in a clockwise direction. If the wind comes from the West, the storm, influenced by the Magnus Effect, will move rapidly north. On the other hand, if the wind originates from the east, the Magnus Effect will propel the rotating air mass to the south.

The Magnus force is a function of geometry, air density, spin rate, and freestream velocity and therefore as the altitude decays, atmospheric density increases thereby increasing the magnitude of this force. As a result, this effect could be significant for spacecraft in the low Ionosphere-Thermosphere region. This added maneuverability without using conventional thrusters could improve efforts to perform in-situ atmospheric research in the low Ionosphere-Thermosphere region. Likewise, this effect can be used to maintain a spacecraft's altitude, and could possibly be used to perform active, controlled deorbiting to improve predictions of the impact location. Thus, this study investigates the feasibility of using the Magnus effect to sustain a spacecraft's orbit at a low perigee altitude of 80km.

### A. Problem Description

A spinning body creates a nonsymmetrical flow pattern (above and below the body) that generates a Magnus effect that yields an aerodynamic lift. As fluid flows past a rotating body, streamlines on the side moving in the same direction as the flow will converge, indicating a diminished pressure [4]. The streamlines on the opposite side move against the freestream and as a result, become more widely spaced, indicating an increase in pressure as shown in Fig. 1. This pressure differential causes a lifting force that will displace the body in a direction normal to the freestream flow. As a result of the dependence on density, the expression for the Magnus force is different for the continuum and free-molecular regime.
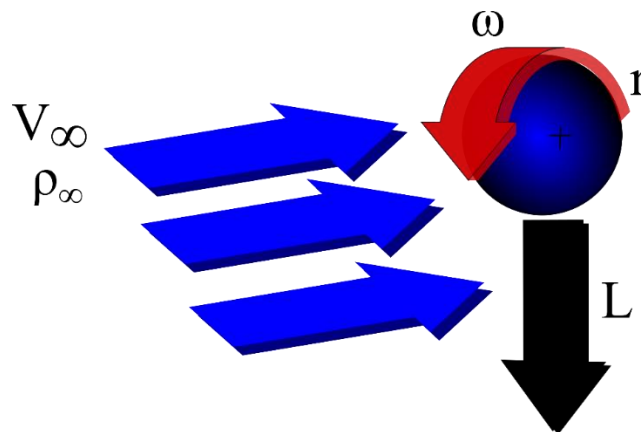


**Figure 1. Lift on a Rotating Body in a Fluid Medium**

American Institute of Aeronautics and Astronautics

A continuum or free molecular regime depends on the mean free path of the fluid. If the mean free path is small in comparison with the dimensions of the body then the fluid can be considered a continuum. With this assumption, the fluid's density, temperature and velocity has a definite value at each point in space. However, many modern engineering applications, including those for spaceflight, occur at high altitudes where the mean free path is not negligible when compared with the dimension of the body and therefore the effects of the discrete character of the fluid must be taken into account when defining its properties [5]. At these two different regimes, the governing physics and interaction of the molecules are different. A widely recognized parameter that determines whether a fluid medium is a continuum or free molecular is the Knudsen number ($K_n$), which is the ratio of the mean free path and the macroscopic length scale of the physical system. In other words, the local Knudsen number is a measure of the degree of rarefaction of a gas [6]. As the local Knudsen number increases, free molecular effects become more pronounced and eventually the continuum assumption breaks down. As the local Knudsen number decreases as a result of the increase in atmospheric density, the Magnus lift becomes more pronounced thereby enhancing the effect of a potential Magnus maneuver. As a result, the work performed in this study is restricted to a spacecraft flying at a perigee of 80km with the objective of investigating the feasibility of the Magnus effect in sustaining the altitude. The magnitude of this force on the orbital decay will be examined by varying the altitude of apogee, spin rate, and mass for a spherical spacecraft having an initial mass of 25kg and a radius of 1m. Continuum and free-molecular theory will be used to formulate the appropriate force as a function of the altitude.

## B. Motivation

Potential applications that intend to also use a lift perturbation to alter the spacecraft's trajectory include satellites or space planes, which will use an airfoil in the hypersonic flow regime to maneuver in Earth's atmosphere. These airfoils can be used for orbit maintenance by providing a lift vector normal to the orbit's velocity vector. Thereby, active altitude adjustments using the proposed Magnus effect on a spinning spacecraft could serve as an orbital maneuver capability without requiring conventional thrusters. For example, the added maneuverability of the Magnus force can possibly allow the spacecraft to perform a *skip reentry*. This reentry technique involves one or more successive *skips* off the atmosphere to achieve greater entry range or to reduce the velocity of the spacecraft before final entry, which helps dissipate the heat at the surface. For entry vehicles with a relatively low lift to drag ratio, a known strategy since the Apollo era for achieving long downrange is to allow the vehicle to skip out of the atmosphere [7]. In addition, the Magnus phenomenon could be used to maintain a low perigee orbit and aid in performing in-situ atmospheric research in the low Ionosphere-Thermosphere region. This could be significantly more effective for planets with higher atmospheric densities including Venus whose atmosphere is mostly made up carbon dioxide. The scenario of perigee maintenance allows for immediate benefits for Operationally Responsive Space (ORS) and Space Reconstitution (SR) missions [8]. Significantly, to perform in-situ research at low perigee altitudes, a substantial propulsion system would be needed to raise and lower the perigee [9]. The Magnus maneuver could meet these requirements.

Equally important, the Magnus effect could be used to perform active, controlled deorbiting to improve predictions of the impact location. This could benefit satellites near EOL, or for systems that fail to fully demise during reentry allowing for a controlled deorbiting capability. For example, several events have previously occurred that illustrate the importance of predicting the reentry location a priori. For example, in the article titled *Assessing the Aviation Risk from Space Debris and Meteoroids* from the Space Safety Magazine it is explained how the uncontrolled reentry of Russia's Phobos-Grunt resulted in the closing of the European airspace for two hours. Most importantly, a study conducted by the FAA following the disintegration of space shuttle Columbia in 2003, found that the probability of an impact between Columbia debris and a general aviation aircraft was one in a hundred [10]. According to the Aerospace Corporation, there are about 100 large man-made objects that reenter the earth's atmosphere uncontrolled each year [10]. Furthermore, if the predicted risk of human casualties exceeds a specified limit, typically .01% per reentry event, a controlled reentry with prescribed reentry location has to be carried out [11]. Similarly, for satellites partially surviving the reentry process, destruction will occur forming a debris cloud where the time to impact the ground or to reach the airspace can be short, as shown in Figure 2. Thus, there exists a need for improving knowledge of the reentry impact location to mitigate the risk of collision between space debris and other ground stations, which could possibly be achieved using the Magnus force.
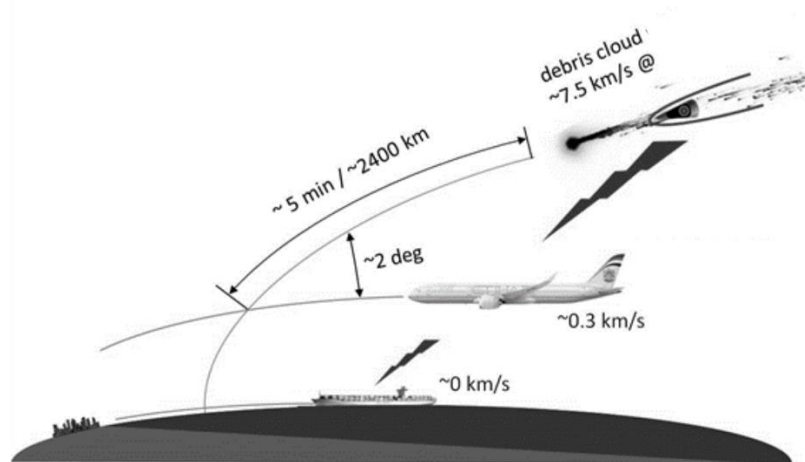
American Institute of Aeronautics and Astronautics

**Figure 2. The risk of collision between space debris and other ground stations** [12]**.**

## II.    Literature Review

A literature review was first conducted to examine how an aerodynamic lift perturbation affects a satellite's orbit. Ashenberg in [13] presents solutions for a flat-plate satellite experiencing non-constant aerodynamic coefficients by using the Gaussian form for the Variation of Parameter (VOP) equations. He describes that if a satellite has dominant flat surfaces, rotates at certain slow rates, or has a large area to mass ratio, the lift forces do not average out to zero. The lift perturbation is considered as a vector in the plane normal to the velocity pointing in any direction. The perturbations are projected in the normal direction given by **h**x**V** toward the inside of the orbit and calculations are done assuming free molecular, hyperthermal flow. The orbit angular momentum is described by **h** whereas **V** is the relative velocity of the satellite. He describes how the lift acting in the orbital plane perturbs the eccentricity vector, while an orthogonal (out-of-plane) force perturbs the orientation of the orbital plane. Significantly, he states that since the lifting force does not change the energy, the semi-major axis is perturbed by drag alone. The general conclusion is that time-varying aerodynamic coefficients may cause various forms of secular orbital motion.

Cook [2] explains that one can neglect the aerodynamic force for a satellite undergoing a rapid and uncontrolled tumbling motion for most of their lifetime since the effects of the normal force to the velocity vector is averaged out over one revolution. However, for satellites that remain stabilized for long intervals of time, one must reexamine the effect of the aerodynamic lift. He assumes lift acts in the orbital plane and investigates two primary cases for a flat-plate satellite: a constant lift to drag ratio followed by a trajectory that has a negative lift coefficient from perigee to apogee and then a constant positive lift coefficient from apogee to perigee. Similar to Ashenberg, he considers the simplest case of hyperthermal free-molecule flow where the thermal accommodation coefficient $\alpha_\tau = 1$, for which the random thermal motion of the molecules is assumed negligible compared with the satellite's speed. With complete accommodation or with a thermal accommodation coefficient value of 1, the lift to drag ratio will be on the order of 0.05. With no accommodation, Cooke describes that the lift to drag ratio can be high as 2/3 and therefore the importance of lift depends on the nature of the momentum exchange at the satellites surface. Furthermore, Cook goes on to explain that since lift acts perpendicular to the satellite's velocity vector, it can have no effect on the semi-major axis of the orbit. Consequently, one should only be concerned with variations of the eccentricity vector. In order for the orbital inclination to change, a component of force normal to the orbital plane is required [14]. For the constant lift coefficient case, Cook finds that the eccentricity remains constant and the only effect of lift is to rotate the major axis. For the discontinuous lift coefficient case, Cook finds that the only secular perturbation is a decrease in the eccentricity.

Moore [15] also describes how satellites in stabilized attitudes may be subjected to steady or periodic lift giving rise to perceptible perturbations in the orbital elements. He uses the LaGrange equations of motion to study the effects of lift and drag on the orbital elements and states that the precise determination of lift effects require either *in-situ* examination of the gas-surface interaction or detailed analysis of orbital perturbations and spin rate data. He describes the hyperthermal free molecular flow as being where the mean free path of the molecules is very large compared with the dimensions of the satellite and where the molecules have no random thermal motion. Diffuse reflection is

American Institute of Aeronautics and Astronautics

significant at 200km-800km where atomic oxygen predominates and at higher altitudes the reflection mode may theoretically approaches specular reflection.

Hall [16] investigates multiple orbital schemes and maneuvers using electric propulsion along the satellite's velocity vector to determine the feasibility of counteracting the drag force at a perigee of 100km. He describes how elliptic orbits utilizing a very low perigee can facilitate access to the surface and atmosphere at sub-ionosphere altitudes while counteracting drag using continuous electric propulsion. Low perigee orbits has been studies for interplanetary scientific missions and has a significant potential for remote sensing. Similarly, the current efforts in this study is to counteract drag at a low perigee without using conventional thrusters or by using a continuous Magnus effect. Unnecessary consumption of fuel to maneuver the spacecraft for short term objectives may severely constrain the life of the satellite [16].

**C. Aerodynamic Lift on a Spinning Sphere**

Due to the importance of lift on the gas-surface interaction assumption, a literature review was also done to examine the expression for the Magnus force in the free-molecular and continuum regime. At high altitudes in orbit, the Knudsen is $K_n \gg 10$ implying free-molecule flow. However, as the satellite reenters to lower altitudes, the Knudsen becomes $K_n \ll 1$ implying a continuous regime. Wang in [17] determines the aerodynamic forces for free molecular flow over a rotating sphere. Most importantly, he describe that in the free molecular regime, the Magnus force exerts a *negative* lift on the sphere. Expressions are derived for the limiting case of hypersonic free molecular flow. Wang explains that if the temperature of the sphere is cold and the reflection is purely diffusive with complete accommodation, then the velocity of the reflected molecules is so small compared with the freestream that it may be neglected. Volkov [18] investigates the 3D rarefied gas flow past a spinning sphere in the transitional and near continuum flow regimes numerically. Volkov describes that in a rarefied gas flow in the absence of intermolecular collisions, the direction of the Magnus force is opposite to that in a continuum flow at small Reynolds numbers. He describes that the negative lift that occurs in the transitional region is attributable to the increase in the contribution of the normal stresses to the Magnus force with a decrease in the Knudsen number. The difference in the Magnus force direction in the free-molecular and continuum regime implies that in the transitional flow regime the Magnus force depends significantly on the Knudsen number. Moreover, at a certain value of the Knudsen number, this force vanishes. Volkov describes that with a decrease in the Knudsen number, the Magnus lift coefficient should first increase from -4/3 to the maximum value of 2 in the continuum flow regime at small Reynolds numbers and then decrease to the limiting value corresponding to large Reynolds numbers.

Rubinow *et al* [19] calculates the Magnus force in the continuum limit using the Navier-Stokes equations assuming small Reynolds number. It is shown that at small Reynolds numbers, the rotation of the sphere does not affect its drag force coefficient. In addition, Rubinow *et al* states that in the continuum regime at small Reynolds numbers the aerodynamic torque exerted on the spinning sphere is independent of the translational velocity of the sphere relative to the fluid. Thus, performing this literature survey allows one to develop the appropriate expression for the Magnus force in the free-molecular limit and continuum regime. To create a smooth transition between the lift coefficient from -4/3 to the maximum value of 2 as the satellite descends into the atmosphere, the hyperbolic tangent function was used which will be discussed later.

## III.    Orbit Perturbations

To understand the orbital mechanics of satellites in LEO, the equations of motion for the two-body problem must first be examined. The physical motions of each planet was first addressed by Kepler where he summarized that 1) the orbit of each planet is an ellipse with the sun at a focus, 2) the line joining the planet to the sun sweeps out equal areas in equal times, and 3) the square of the period of a planet is proportional to the cube of its mean distance from the sun [20]. Newton then mathematically explained why planets and satellites followed an elliptical orbit by combining his *Law of Universal Gravitation* and his *Second Law of Motion* resulting in Eq. (1). This equation describes the satellite's position vector as it orbits the earth and assumes that: gravity is the only force acting on the system, the Earth is spherically symmetric, the Earth's mass is much greater than the satellite's mass, and the earth and the satellite are the only two bodies in the system [21]. To clarify, $r$ is the position of the satellite relative to Earth's center and this differential equation is a second order, nonlinear, differential equation.

$$\ddot{\mathbf{r}} + (\mu r^{-3})\mathbf{r} = 0 \tag{1}$$

A solution to the two-body equation of motion for a satellite orbiting earth is the polar equation of a conic section [21]. In order to solve Eq. (1) six constants of integration or initial conditions are required and thus one can define the

American Institute of Aeronautics and Astronautics

orbit with six classical orbital elements with one quantity varying with time as shown in Fig. 3. A spacecraft's orbit or trajectory is its path through space and an orbit is specified by a state vector which can be the position and velocity of the spacecraft.
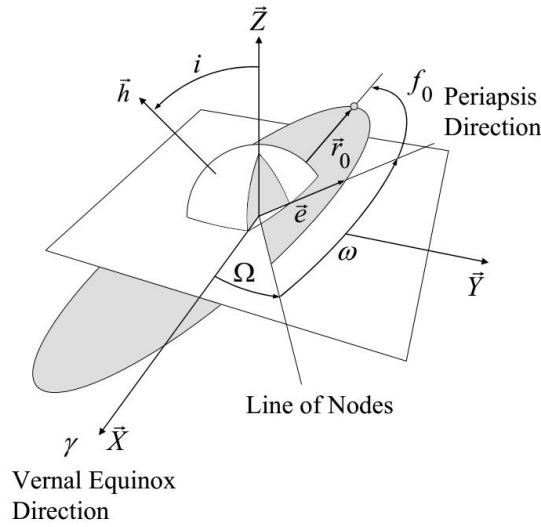


**Figure 3. Keplerian orbital elements of a satellite in an elliptic orbit** [21]**.**

A brief summary of the classical orbit elements as described in [21] includes:
- *Semi-Major Axis (a)*: defines the size of the orbit
- *Eccentricity (e):* defines the shape of the orbit
- *Inclination (i):* the angle between the angular momentum vector $\vec{h}$ and unit vector $\vec{Z}$.
- *Right Ascension of the Ascending Node (RAAN Ω):* The angle from the vernal equinox to the ascending node. The ascending node is the point where the satellite passes through the equatorial plane moving from south to north.
- *Argument of Perigee(ω):* The angle from the ascending node to the eccentricity vector measured in the direction of the satellite's motion. The eccentricity vector points from the center of the earth to perigee with a magnitude equal to the eccentricity of the orbit.
- *Mean anomaly (M):* The fraction of an orbit period which has elapsed since perigee expressed as an angle. The mean anomaly equals the true anomaly for a circular orbit.

## D. Equations of Motion with Perturbations

A satellite will always remain in orbit and consequently its orbital elements will remain constant if gravitational forces are the only force acting on it. However, when other perturbations are present, the two-body problem becomes Eq. (2) implying that orbital lifetime becomes finite,

$$\ddot{\mathbf{r}} + \frac{\mu}{r^3}\mathbf{r} = \mathbf{a_P}$$

(2)

where $a_P$ is the resultant vector of all the perturbing accelerations. Some of these perturbing acceleration terms include atmospheric drag, solar radiation pressure, Earth's oblateness, and other (n-body effect) [20]. In the solar system, the sum of the perturbing accelerations for all satellite orbits is at least 10 times smaller than the central force or two-body accelerations or $a_P << \frac{\mu}{r^3}$ [22]. The non-homogenous equation above implies that the semi-major axis $a$, orbit angular momentum $h$, and eccentricity $e$ are not constants but satisfy [2],

American Institute of Aeronautics and Astronautics

$$\dot{a} = \frac{2a^2}{\mu}\dot{\mathbf{r}} \cdot \mathbf{f} \qquad (3)$$

$$\dot{h} = \mathbf{r} \times \mathbf{f} \qquad (4)$$

$$\dot{e} = \frac{1}{\mu}\{\mathbf{h} \times \mathbf{f} + (\mathbf{r} \times \mathbf{f}) \times \dot{\mathbf{r}}\} \qquad (5)$$

Due to the non-linear nature of Eq. (2) with respect to $r$, no closed form analytical solution exists and therefore it must be solved numerically to obtain $r(t)$ and $\dot{r}(t)$ as functions of time.

### E. Methods of Solution

A perturbation is a deviation from the Keplerian motion and includes secular and periodic perturbations. Secular perturbations are those which the effects build up over time while periodic or cyclic perturbations are such that the effects cancel after one cycle or orbit [22]. Furthermore, secular changes in a particular element very linearly over time or proportionally to some power of time. Periodic perturbations are either short or long term where short periodic typically repeats on the order of the satellite's period or less and long periodic effects have cycles considerably larger than one orbit period [22]. Even in the absence of perturbations, *fast* variables which change considerably during one revolution, include the mean, true, and eccentric anomalies. However, slow variables including semi-major axis, eccentricity, inclination, node, and argument of perigee change very little during one revolution [23]. If there is no perturbations, all the *slow* variables would remain constant. The largest perturbation is due to gravitation, followed by drag, third body perturbations, solar radiation pressure effects, and smaller effects such as tides. Third body effects are perturbations caused by the attraction of the sun, moon, and other planets. In addition, solar radiation pressure is when photons impact a satellite's surface and are reflected or absorbed.

Techniques to solve the two-body problem with perturbations encompass analytical and semi-analytical methods. In using these methods, the primary difference is whether one uses the satellite's position and velocity state vectors or the orbital elements as the elements of state. Typically analytical methods are faster but the expressions are truncated to allow simpler expressions. As a result, the computational speed increases but accuracy decreases. Numerical approaches consists of numerically integrating the perturbing accelerations. The numerical approach can also be applied to the Variation of Parameter (VOP) equations in which case a set of orbital elements are numerically integrated [22].

Furthermore, the three main methods to solving the equations of motion with perturbations are special perturbation, general perturbation and semi-analytic. Special perturbation techniques including Cowell's method and Encke's method, uses numerical integration of the equations of motion including all perturbing accelerations [22]. This approach uses the position and velocity vectors of the satellite. However, the analytical approach uses the orbital elements for integration while semi-analytic methods uses a combination of numerical and analytical techniques. Most analytical and a few numerical approaches use the VOP form of the equations since the orbital elements in the two-body equation are changing. Lagrange and Gauss both developed VOP methods to analyze perturbations. Lagrange's technique applies to conservative accelerations while Gauss's approach can also be implemented for non-conservative accelerations. Conservative accelerations are explicitly a function of position only and there is no net transfer of energy taking place and therefore the mean semi-major axis of the orbit is constant. However, non-conservative accelerations are explicitly a function of both position and velocity including atmospheric drag, outgassing, and tidal friction effect where energy transfer occurs thereby changing the semi-major axis. [22]. Drag is a non-conservative force and will continuously reduce the energy of the orbit decreasing the semi-major axis and period. The orbit will become more circular each revolution and will then rapidly spiral inwards due to the dense atmosphere. Using the VOP technique, one can examine the effects of perturbation on specific orbital elements. In the Gaussian VOP, the rates of change of the elements are explicitly expressed in terms of the disturbing forces. Since a low perigee of ~80km will be examined, the dominating perturbing force will be from drag and the Magnus effect allowing one to ignore other perturbations. Significantly, one can see that the Magnus force will change as a function of time since it primarily depends on the atmospheric density classifying it as a secular, non-conservative force.

American Institute of Aeronautics and Astronautics

# IV. Implementation of Software

Numerical propagation of a satellite's trajectory using the Magnus effect would consist of many interacting components including: a numerical propagator that solves the equation of motion and a force model that evaluates the effect of the Magnus force on the satellite. Since the current study is examining the feasibility of the Magnus force, we decided to model its effect as a super-efficient thruster for simplicity. The Systems Tool Kit (STK) allows the user to incorporate customer specific modeling into the computations by creating a plugin, which provide a simple method for customizing STK. The equations of motion are integrated using the Runge-Kutta-Fehlberg method of 7th order with 8th order error control [16]. However, before beginning to perform the simulations, a test case was performed to verify that the software implementation was correct. The simulation validation case was taken from Hall [16], whom used STK to examine the final altitude for a constant initial perigee altitude of 100km with an increasing apogee altitude between 2,622km to 18,622km. A 150mN of continuous thrust was fired along the velocity vector from perigee to apogee. The satellite was then allowed to coast back to perigee without the use of any thruster and this sequence was repeated 100 times. As shown in Figure 4, there is good agreement between the STK simulation and by Hall giving confidence that the software was being executed correctly.
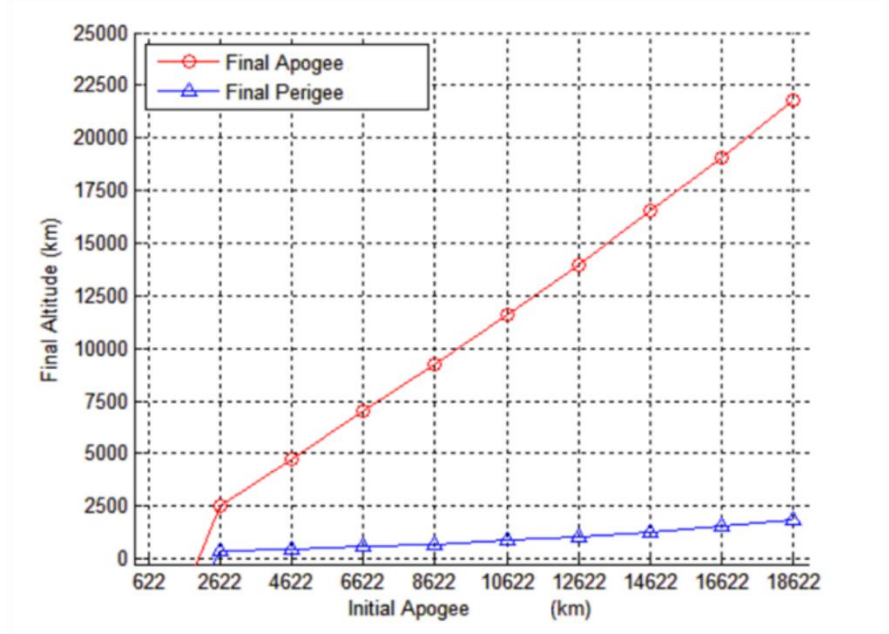
American Institute of Aeronautics and Astronautics
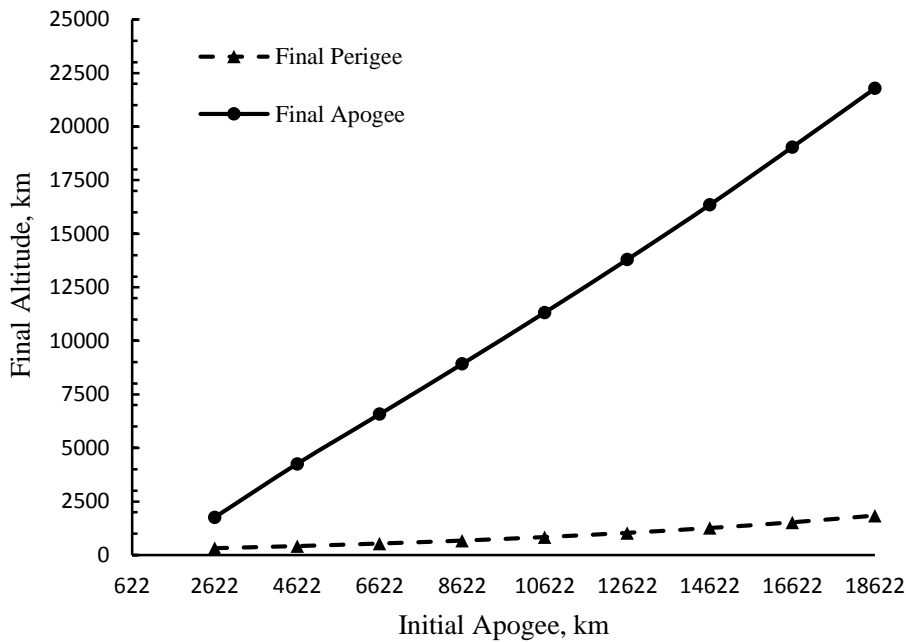
**Figure 4. STK Validation**

### F. Super-Efficient Thruster Model

A plugin component is a user-supplied software component called by the application at certain pre-defined event times within the computation cycle [24]. The plugin is allowed to modify the computation by adding additional considerations or modifying parameters. A custom script is implemented using Visual Basic Scripting (VBS) that pulls in the instantaneous density, altitude, and velocity to evaluate the magnitude of the Magnus force. Ideally, with the real application of this concept the satellite will not be losing any mass. To create a similar effect in STK, an exceedingly high specific impulse of $2 \times 10^{12}$ s was created with a fuel mass of 5kg. Therefore, the mass of fuel consumed for each simulation was negligible, ($\sim 3 \times 10^{-13}$kg), allowing one to approximately model the Magnus effect. Also, theoretically, one does not have the capability to incorporate a high spin rate on the actual satellite in STK. Thus, a spin rate of 5000RPM and radius of 1m is assumed in order to evaluate the magnitude of the Magnus force which is then implemented via a thruster.

Three types of attitude motion include pure rotation, coning, and nutation. The Magnus force is assumed to be in pure rotation, which is the limiting case where the rotation axis, a principal axis, and a geometrical axis are parallel or anti-parallel [25]. As a result, the angular momentum vector will lie along the same axis. Thus, with this assumption the spin axis is assumed to lie perpendicular to the orbital plane resulting in the lift vector acting in the orbital plane. The Magnus force perturbation can be expressed as Eq. (6),

$$\mathbf{F_m} = \frac{1}{2} C_l \pi r^3 \rho_\infty \omega V \ \hat{\mathbf{u}} \quad \text{where} \quad \hat{\mathbf{u}} = \frac{\omega \times \mathbf{V}}{\|\omega \times \mathbf{V}\|} \tag{6}$$

where $r$ is the radius of the sphere, $\omega$ is the angular velocity, $V$ is the freestream velocity, and $\rho$ is the freestream density. The lift coefficient for the Magnus force, as described by [18], [4], and [17], is negative in the free molecular regime and depends on $\alpha_\tau$, the momentum accommodation coefficient as shown below in Eq. (7).

$$C_l = \frac{-4}{3} \alpha_\tau \tag{7}$$

To ensure that the Magnus force is always perpendicular to the satellite's velocity vector, a new reference frame was defined for the Magnus force that is based on the cross product of the velocity of the satellite $\vec{V}$ and its orbit angular

9

American Institute of Aeronautics and Astronautics

momentum $\vec{h}$. Please refer to the appendix which demonstrates that the orbit angular momentum is significantly greater than the satellite's body angular momentum for a spin rate of 5000RPM.

To create a realistic model and a smooth transition between the changing lift coefficients as the satellite's trajectory descended from a free molecular regime to continuum regime, the hyperbolic tangent function was used. However, in order to decide what approximate altitudes the Magnus lift would change from negative to positive, the Knudsen number was first calculated using the expression below in Eq. (8) taken from [26],

$$K_n = \sqrt{\frac{\pi}{2RT}} \frac{\mu}{\rho D} \tag{8}$$

where, $\mu$ is the dynamic viscosity, $R$ is the specific gas constant, $D$ is the diameter of the sphere, and $T$ is the temperature at a given altitude. At altitudes higher than 100km, free molecular conditions will prevail or when $K_n >$ ~10. Subsequently, the flow will move into transition flow as the Knudsen number decreases in the range of $0.1 < K_n$ <10 and then into slip flow where the no-slip boundary condition starts to break down or when $0.001 < K_n < 0.1$. Examining Table 1, one can see that the continuum regime starts around ~80km or where $K_n < ~ 0.001$ assuming a satellite radius of 1m. As stated previously, Volkov [18] describes that with a decrease in the Knudsen number, the value of $C_l$ should first increase from -4/3 to the maximum value of 2 corresponding to the continuum flow regime at small Reynolds number. As a conservative approach, the limiting case of hypersonic free molecular flow is assumed and therefore the reflection is purely diffusive with complete accommodation ($\alpha_\tau = 1$) [27]. With a purely diffusive assumption as opposed to a specular reflection, the lift is small compared to drag and results in a conservative approximation for the Magnus force.

**Table 1**. Knudsen number at varying altitudes

| Altitude, km | $K_n$ |
|:---:|:---:|
| 100 | 0.0619 |
| 86 | 0.0049 |
| 80 | 0.0019 |
| 70 | 0.0004 |
| 66 | 0.0005 |

*1. Hyperbolic Tangent Function*

After calculating the altitude where continuity conditions prevailed, the hyperbolic tangent function was developed to create a smooth transition from the negative lift coefficient to the positive lift coefficient in the continuum regime as described by the literature. The developed function can be seen in Eq. (9) and Fig. 5, where $x$ is the altitude of the satellite.

$$C_L = \frac{1}{3} - \frac{5}{3} * \tanh(2 \cdot x - 164) \tag{9}$$

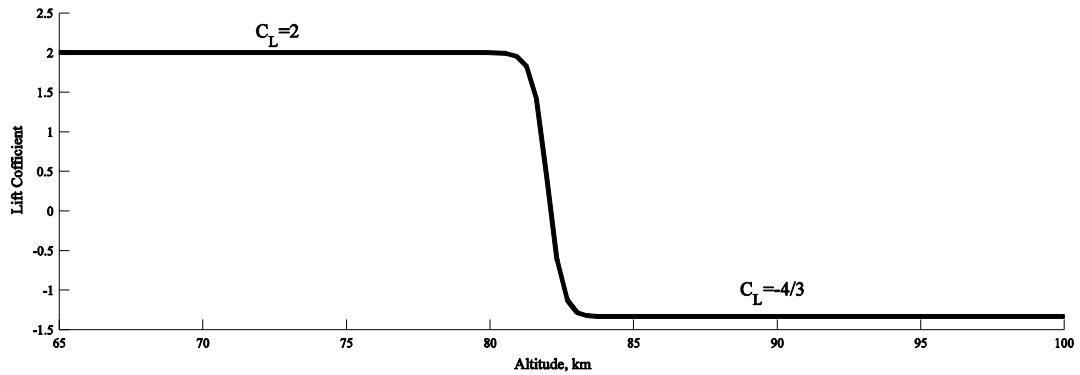American Institute of Aeronautics and Astronautics

**Figure 5. Hyperbolic Tangent Function creates a transition between Positive and Negative Magnus Lift.**

Thus, the super-efficient Magnus engine plugin is implemented using Eq. (6), which evaluates the Magnus lift coefficient based on the instantaneous altitude of the satellite in STK as seen in Eq. (9). As a result, the custom script developed using Visual Basic Scripting (VBS) pulls in the instantaneous density, and the altitude and velocity of the satellite in order to evaluate the magnitude of the Magnus force described in Eq. (6).

*2. STK Astrogator Settings*

In the STK graphical user interface, coefficients for solar radiation pressure are set to zero. Drag is incorporated into the simulations and is based upon the Jacchia-Roberts Atmospheric density model. The coordinate system used in the simulations is the VNC (Velocity-Normal-Conormal) reference frame. In this frame, the X-axis is along the velocity vector **V**, the Y-axis is along the orbit normal or Y =**r**x**V**, and the z-axis completes the orthogonal triad. The orbit epoch time is set to October 4th, 2012 12:00. The Magnus thruster is modeled as a finite maneuver which is effectively a propagate segment with thrust. It uses the defined propagator to propagate the state accounting for the acceleration due to thrust. Each point calculated during the numerical simulation is added to the satellite's ephemeris until a stopping condition is met [28]. In STK's Astrogator, two finite maneuvers are implemented with the custom engine plugin to account for the change in the Magnus lift coefficient as the satellite descends from a free molecular regime to a continuum regime. Initially the satellite is not in the continuum regime (≥84km), and thereby the first maneuver puts the Magnus direction as equal to **h**x**V** to account for the negative Magnus force. Under 84km, another finite maneuver is done to implement the thrust acting in the **V**x**h** direction. As previously stated, the mass is set to 20kg with 5kg of fuel defined with a cross sectional area of 3.14m$^2$ assuming a spherical geometry with a radius of 1m. As a note, the mass of fuel needs to be defined in order for STK to perform the simulations even if the fuel consumption is very low. The drag coefficient is set of a value of 2 as described in [17] that is based on the limiting case of hypersonic free molecular flow assumptions, where one assumes the reflection is purely diffusive with complete accommodation ($\alpha_\tau = 1$). Also, for all simulations, a decay altitude of 65km was used.

*3. Correct Implementation of Formula*

Before performing the required simulations, a simple test case was performed to ensure that the custom engine plugin was working correctly. The Magnus thruster was programmed to pull in the atmospheric density, altitude, and the velocity components of the satellite during each time step. After pulling in the velocity components along the X, Y, and Z-axis the magnitude of the velocity vector was found. With an assumed spin rate of 5000RPM and radius of 1m, and using the density and magnitude of the velocity output from STK, one can plot the expected theoretical thrust given by Eq. (6) against the magnitude of the thrust output simulated in STK. Looking at Fig. 6, one can see that the good agreement with the thrust ensures that the user-defined thruster is accurately pulling in the density and velocity as a function of time.
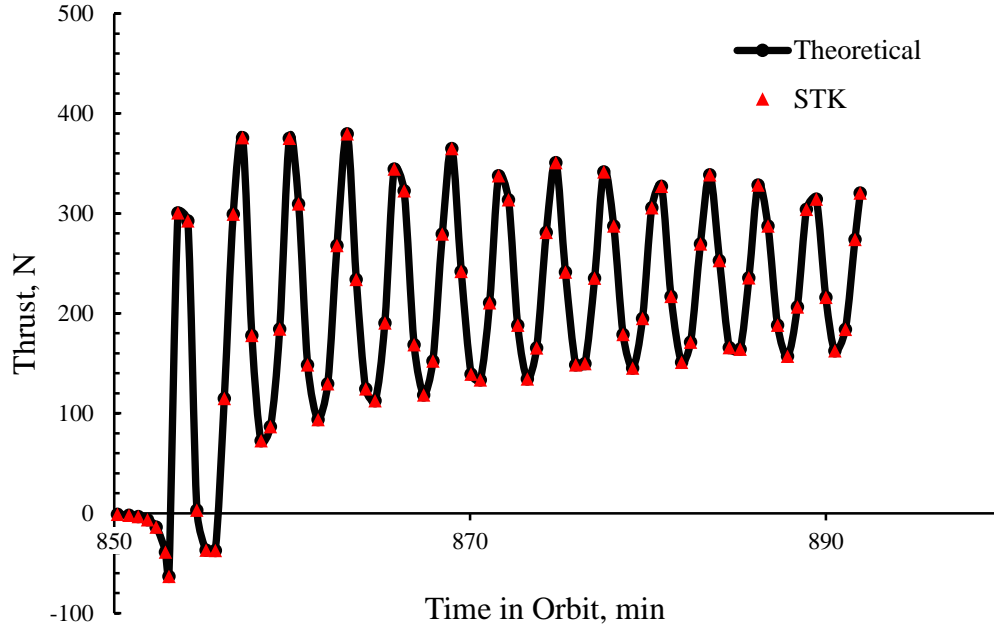
American Institute of Aeronautics and Astronautics

**Figure 6. Verifying Magnus Thruster Implementation is Correct**

In addition, as seen above in Fig. 6, the lift coefficient is initially negative since the satellite is in the free molecular regime. However, as the altitude decreases (<84km) we start to see a rapid increase in thrust and see that the thrust is no longer negative This is expected since the satellite is now in the continuum regime. One can see that the magnitude of the thrust acting on the satellite starts to oscillate as shown in Fig. 6 as a result of the interaction between the drag, gravitational force, and Magnus effect. To clarify, as the satellite descents lower in the atmosphere, the density increases producing a larger Magnus thruster increasing the altitude of the satellite. However, as the altitude increases, the density decreases thereby reducing the effect of the Magnus thruster causing the thrust plot to have a sinusoidal behavior.

**G. Spin Rate Required to Avoid Losing Height**

After verifying that the Super-efficient thruster was being implemented correctly, a simple analysis based on [8] was then performed to examine the spin rate required for the satellite not to lose altitude using the equation for the Magnus lift and drag as seen in Eq. (10) and (11). This rough analysis gives one insight on the spin rate required based on geometry, mass, and altitude. For a conservative approximation, the lift coefficient for a spinning sphere in free molecular flow was used which can be found in [17] and [18],

$$L = \frac{2}{3}\pi r^3 \rho \omega V \qquad (10)$$

$$D = \frac{1}{2}\rho C_d A V^2 \qquad (11)$$

where $r$ is the radius of the sphere, $\rho$ is the density at a given altitude, $\omega$ is the angular velocity of the sphere in rad/s, $V$ is the velocity of the sphere, $C_d$ is the drag coefficient, and $A$ is the reference area. Given a mass of 25kg and a radius of 1m, the angular velocity of the sphere is used as the independent variable in this example. Assuming the

12

American Institute of Aeronautics and Astronautics

satellite travels through the atmosphere with a constant flight path angle of 10°, the required spin rate as a function of different radii at different altitudes can be found using the free body diagram of Fig. 7, where the only assumed forces acting on the satellite are lift, drag, and weight.
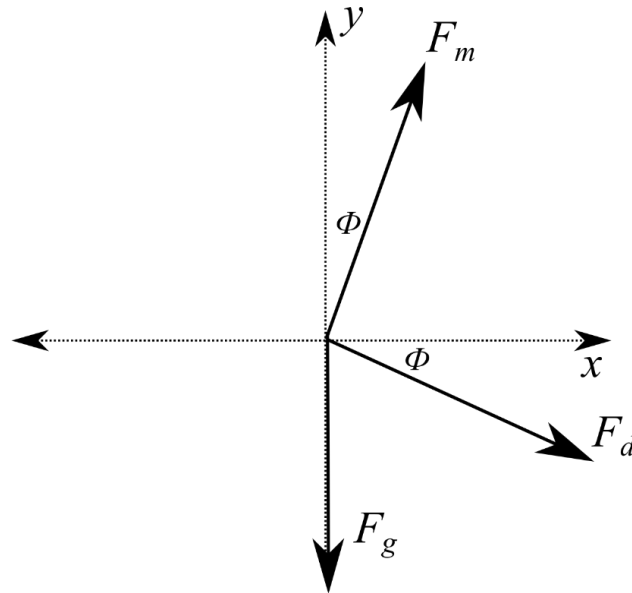


**Figure 7. Simplified Magnus Force Analysis in a Continuum Regime**

Using the 1976 Standard Atmosphere Model, a velocity of 7.5km/s, and a constant mass of 25kg, the required spin rate to avoid losing altitude is calculated by summing the forces in the $x$ and $y$ direction for different altitudes and is plotted in Fig. 8. As the angular velocity increases, the radius required to produce the required lift to avoid losing altitude decreases. Also, as the altitude increases, the resulting low density requires an exceedingly large radius to generate the required lift. Examining this simple analysis, might encourage one to believe that the Magnus effect is impractical due to the high required spin rates. However, this study will demonstrate that in a low perigee altitude of 80km, a spin rate of 5000RPM, and a 1m radius sphere is sufficient for delaying the reentry period assuming a decay altitude of 65km.
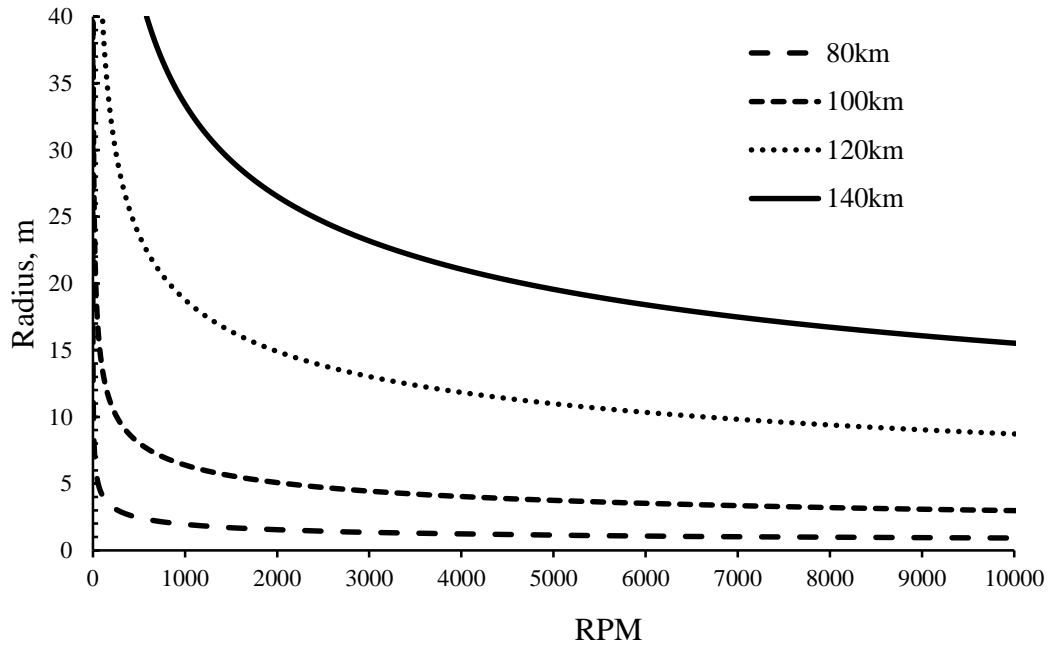
American Institute of Aeronautics and Astronautics

**Figure 8. Angular velocity and radius required to avoid losing height.**

## V. Results

To investigate the feasibility of using the Magnus effect on a spinning spacecraft to prolong its trajectory in a regime of considerable density, we decided to first vary the altitude of apogee while keeping the altitude of perigee at 80km. Subsequently, the next step involved changing the magnitude of the Magnus thruster by theoretically increasing the rotational speed of the satellite. Finally, a simulation is conducted at different masses to examine the effect on the feasibility of the Magnus effect.

### H. Maintaining Altitude of Perigee

Performing initial simulations in STK demonstrated that the Magnus effect was only effective at altitudes around 80km due to the increase in atmospheric density. Thus, the first analysis examined the effect of holding the altitude of perigee constant at 80km while increasing the altitude of apogee or eccentricity of the orbit as shown in Table 2.

**Table 2. List of Orbital Elements for an Altitude of Perigee = 80km**

| Apogee Altitude | e | i | Ω (deg) | ω (deg) | M (deg) |
|---|---|---|---|---|---|
| 145.18 | 0.005 | 40 | 0 | 0 | 180 |
| 177.88 | 0.008 | 40 | 0 | 0 | 180 |
| 210.74 | 0.010 | 40 | 0 | 0 | 180 |
| 411.46 | 0.025 | 40 | 0 | 0 | 180 |
| 760.08 | 0.050 | 40 | 0 | 0 | 180 |
| 1127.54 | 0.075 | 40 | 0 | 0 | 180 |
| 1515.42 | 0.100 | 40 | 0 | 0 | 180 |
| 2359.62 | 0.150 | 40 | 0 | 0 | 180 |

American Institute of Aeronautics and Astronautics

| 3309.34 | 0.200 | 40 | 0 | 0 | 180 |
|---|---|---|---|---|---|
| 4385.70 | 0.250 | 40 | 0 | 0 | 180 |

Examining the results in Fig. 9, one can see that using 65km as the decay altitude, the Magnus effect approximately doubles the amount of time in orbit assuming a spin rate of 5000RPM. Therefore, there might be the possibility that the Magnus effect could counteract drag at a low perigee without using conventional thrusters. This extension of time on orbit could possibly be used by a spacecraft to maneuver itself to an area that will reduce the impact of collisions with the airspace. Likewise, the extension of time on orbit could be used to maintain a low perigee orbit and aid in performing in-situ atmospheric research in the low Ionosphere-Thermosphere region. Significantly, this could be more effective for planets with higher atmospheric densities.
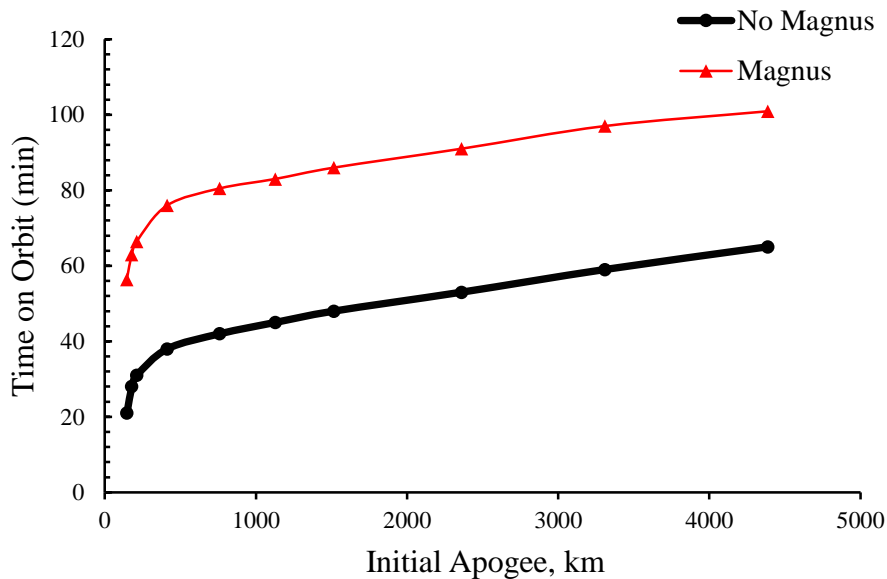


**Figure 9. Amount of time on orbit, with and without Magnus Thruster at 80km Perigee.**

## I. Different RPM

Next, the effect of changing the angular velocity in Eq. (6) was performed to see the effect on the time in orbit. The first set of orbital parameters in Table 2 (apogee=145.18km, e=0.005) was chosen as the set to be analyzed. Examining Fig. 10, without the Magnus thruster, the time in orbit is around 20min. However, with the Magnus Thruster enabled with a spin rate of 5000 RPM, the time in orbit until decay is extended to 60min. Furthermore, as the spin rate is increased to 10,000 RPM no decay is seen in the orbit within the allotted 20,000min simulation time and the satellite is seen to oscillate at an altitude of 66km.
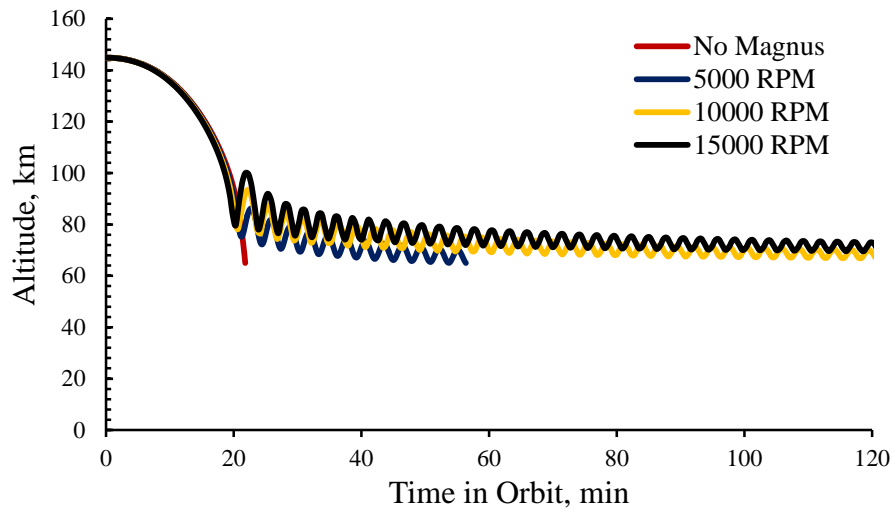
American Institute of Aeronautics and Astronautics

**Figure 10. Time in Orbit for Different Spin Rates**

The behavior of Fig.10 is expected as the RPM is increased if one reexamines Fig. 8, (which is replotted in Fig. 11 for clarity). For a satellite with a radius of 1m, Fig. 11 illustrates that a spin rate of at least 7000RPM or above is required to not lose height for an altitude of 80km. Thereby, one can see that the spin rate of 10,000RPM-15000RPM is over the required minimum of 7000RPM and thus the satellite's altitude oscillates and the STK simulation time is over the time limit threshold of 20,000min. The Magnus force magnitude is able to overcome the drag and weight force contribution.
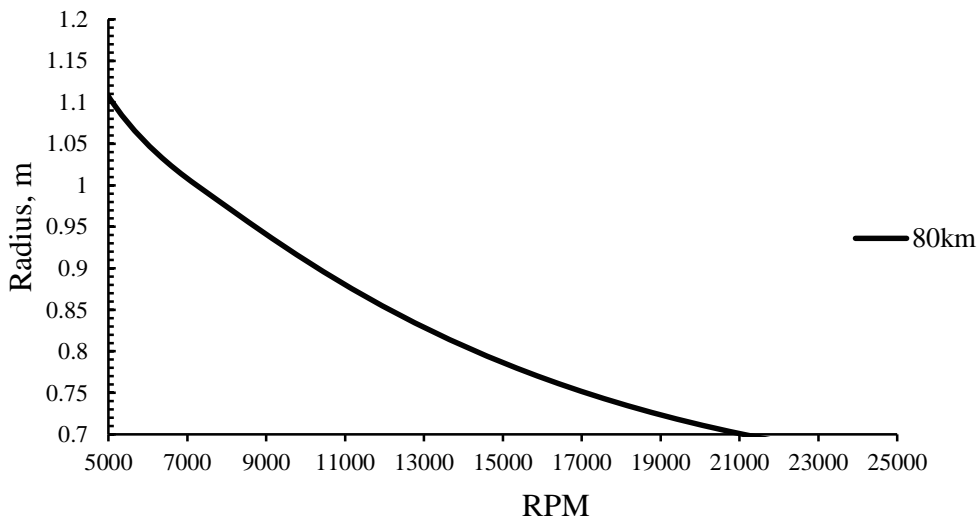


**Figure 11. Minimum radius required to not lose altitude at a given angular velocity.**

**J. Different Mass**

The last parameter that was changed was the total mass of the spacecraft. Examining Fig. 12, for a spin rate of 5000RPM, the satellite with 10kg mass oscillates at an altitude of 67km and the lifetime is over 20,000min. However,

American Institute of Aeronautics and Astronautics

the 25kg satellite's lifetime is ~56min and the 50kg satellite is ~43min. From a design perspective, in order to use the Magnus force effectively, one should reduce the mass and increase the radius.
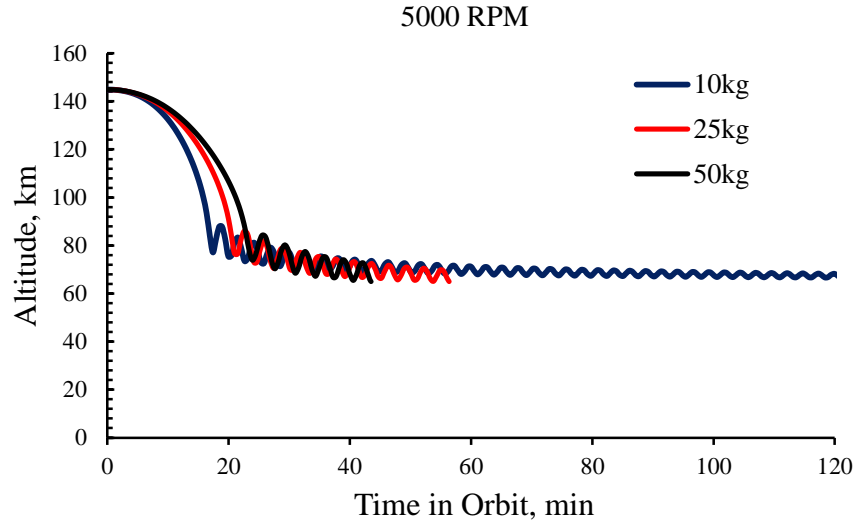


**Figure 12. Time in Orbit for different masses.**

## VI.    Generating Spin Rate

A way to generate the required spin rate is now briefly reviewed. As stated in the literature review, Rubinow *et al* states that in the continuum regime at small Reynolds numbers the aerodynamic torque exerted on the spinning sphere is independent of the translational velocity of the sphere relative to the fluid. In addition, Rubinow *et al* presents a relationship for the torque on the sphere as shown in Eq. (12).

$$T = -8\pi\mu r^3 \omega \qquad (12)$$

Using a spin rate of 5000RPM, with a radius of 1m, the required torque to spin can be found in Table 3 using the viscosity of air from the 1976 Standard Atmosphere model. Assuming an average required torque of 0.17 N·m, one possible way to generate this torque could be to use reaction wheels. For example, Blue Canyon Technologies' RW8 generates a max torque of 0.11 N·m and HoneyBee Robotic's Microsat CMG generates a torque of 0.172 N·m [29], [30].

**Table 3**. Required Torque at varying altitudes

| Altitude, km | Torque, N·m |
| --- | --- |
| 65 | -0.20 |
| 70 | -0.19 |
| 80 | -0.17 |
| 86 | -0.16 |

American Institute of Aeronautics and Astronautics

## VII.    Conclusion

This study involved modeling the Magnus Effect as a super-efficient thruster in STK for a spherical spacecraft with a total mass of 25kg and cross sectional area of 3.14m$^2$. The magnitude of this force on the orbital decay was examined by varying the altitude of apogee, spin rate, and mass. Assuming a decay altitude of 65km with a perigee of 80km, it was seen that the Magnus effect doubles the amount of time in orbit assuming a spin rate of 5000RPM. As the spin rate increased, it was seen that at 10000RPM and 15000RPM, the satellite's altitude oscillates and did not decay within the 20,000min simulation time. Furthermore, as we reduce the mass, the Magnus force is seen to be more effective since the gravitational force will be smaller. This preliminary analysis demonstrated that the Magnus effect has the potential to sustain a spacecraft's orbit at a low perigee altitude and could serve as an orbital maneuver capability. This research can provide insight to new technologies including the capability of performing a *skip* reentry helping the spacecraft to achieve a greater entry range or assist in dissipating the heat from the surface. Equally important, a controlled deorbiting to improve predictions of the impact location using the Magnus maneuver could be a possibility. The additional time in orbit gained by the Magnus effect could aid in performing in-situ atmospheric research in the low Ionosphere-Thermosphere region. This could be significantly more effective for scientific missions on planets with higher atmospheric densities including Venus whose atmosphere is mostly made up carbon dioxide. In addition, it was shown that with the torque requirements to generate the necessary spin, reaction wheels or CMG's could be appropriate. However, this was only a feasibility study examining the magnitude of the Magnus force in the free molecular and continuum regime and is a prelude to a more detailed design project where other trade-off studies will be performed. For example, an aerothermal analysis must be performed examining the material selection and the hypersonic air flow interaction with a spinning satellite. Also, a full description on the hardware requirements on how to spin the sphere and material selection will be done in future work.

## VIII.    Appendix

### K. Body vs. Orbit Angular Momentum Calculations

Here we perform the calculations for the satellite's body angular momentum and compare it with the orbit angular momentum. We perform the calculation for a circular orbit with a semi-major axis of 6490.59km for a satellite mass of 25kg with a radius of 1m.

### 4. *Orbit Angular Momentum*

Assuming the orbit to be circular the orbital angular momentum can be expressed as,

$$\vec{\mathbf{L}} = m_e r^2 \omega_{orbit} \, \hat{\mathbf{k}} \tag{13}$$

where $r$ is the radius of the orbit and $\omega_{orbit}$ is the orbit angular velocity. To find the orbital angular velocity we use,

$$\omega_{orbit} = \frac{2\pi}{T_{orbit}} \tag{14}$$

Lastly, to find the time of orbit or $T_{orbit}$, we use,

$$T_{orbit} = 2\pi\sqrt{\frac{a^3}{\mu}} = 2\pi\sqrt{\frac{(6490.59x10^3 m)^3}{3.98x10^{14}\frac{m^3}{s^2}}} = 5203\text{s} \tag{15}$$

As a result, the orbital angular velocity is found to be 0.00120 rad/s. Using Eq. (13) the orbit angular momentum is found to be,

$$\vec{\mathbf{L}} = 25kg \cdot (6490.59x10^3 m)^2 \cdot 0.00120\frac{rad}{s} = 1.27160x10^{12} \, kg \cdot m^2 \cdot s^{-1} \, \hat{\mathbf{k}}$$

### 5. *Body Angular Momentum*

We assume we have a spherical satellite and approximate it as a uniform sphere. As a result, the moment of inertia of the satellite about its center of mass is,

American Institute of Aeronautics and Astronautics

$$I_{cm} = \frac{2}{5} m_e R_e{}^2 \tag{16}$$

where, $m_e$ and $R_e$ is the mass and radius of the satellite. The body angular momentum can then be found using,

$$\vec{\mathbf{L}} = I \cdot \omega_{spin} = \frac{2}{5} m_e R_e{}^2 \omega_{spin} \, \hat{\mathbf{n}} \tag{17}$$

where $\hat{\mathbf{n}}$ is a unit vector pointing along the axis of rotation of the satellite. Assuming we are spinning at 5000RPM or 523 rad/s the body angular momentum is found to be,

$$\vec{\mathbf{L}} = I \cdot \omega_{spin} = \frac{2}{5} \cdot 25kg \cdot 1m^2 \cdot 523\frac{rad}{s} = 5230 \; kg \cdot m^2 \cdot s^{-1} \; \hat{\mathbf{n}}$$

Thus, the orbit angular momentum is found to be millions of times greater than the satellite's body angular momentum.

## IX.     References

[1]     C. L. Pulido, "Aerodynamic Lift and Drag Effects on the Orbital Lifetime Low Earth Orbit (LEO) Satellites," University of Colorado Boulder .

[2]     G. E. Cook, "The Effect of Aerodynamic Lift on Satellite Orbit," *Plant. Space Science* , vol. 12, p. 11, 1964.

[3]     K. I. Borg, L. H. Soderholm and H. Essen, "Force on a Spinning Sphere Moving in a Rarefied Gas," *Physics of Fluids,* vol. 15, no. 3, pp. 736-741, 2003.

[4]     J. Borg, "Magnus Effect: An Overview of its Past and Future Practical Applications," NAVSEA , Washington D.C., 1986.

[5]     H.-S. Tsien, "Superaerodynamics, Mechanics of Rarefied Gases," *Journal of the Aeronautical Sciences,* vol. 13, no. 12, pp. pp. 653-664, 1946.

[6]     S. Roy, R. Raju, H. F. Chuang, B. A. Cruden and M. Meyyappan, "Modelng Gas Flow Through Microchannels and Nanopores," *Journal of Applied Physics* , vol. 93, no. 8, p. 10, 2003.

[7]     P. Moseley, "The Apollo Entry Guidance: A Review of the Mathematical Development," in *TRW Note No. 69-FMT-791*, Houston, TX, 1969.

[8]     M. N. Goodson, "Applications of Aerodynamic Forces for Spacecraft Orbit Maneuverability in Opereationally Responsive Space and Space Reconstitution Needs," Air Force Institure of Technology, Ohio, 2012.

[9]     M. A. Mesarch, "Orbit Optimization For The Geospace Electrodynamics Connections (GEC) Mission," American Institute of Aeronautics and Astronautics , 2003.

[10]     M. Emanuelli and T. Sgobba, "Assessing the Aviation Risk from Space Debris and Meteoroids," *Space Safety Magazine,* no. 8, p. 32, 2013.

[11]     R. Janovsky, M. Kassebom, H. Burkhardt, M. Sippel, G. Krulle and B. Fritsche, "End of Life De-orbiting Strategies for Satellites," 2002.

[12]     S. Ramjatan, T. Magin, T. Scholz, V. van der Haegen and J. Thoemel , "Blackout Analysis of Small Cone-Shaped Reentry Vechicles," *Journal of Thermophysics and Heat Transfer,* [Accepted for Publication].

[13]     J. Ashenberg, "On the Effects of Time-Varying Aerodynamics Coefficients on Satellite Orbits," *Acta Astronautica* , vol. 38, no. 2, pp. 75-86, 1996.

[14]     G. E. Cook and R. Plimmer, "The Effect of Atmospheric Rotation on the Orbital Plane of a Near-Earth Satellite," in *Proceedings of the Royal Society of London. Series A, Mathematical and Physical Sciences* , Farnborough, 196.

[15]     P. Moore, "The Effect of Aerodynamic Lift on Near-Circular Satellite Orbits," *Planet, Space Sciences* , vol. 33, no. 5, pp. 479-491, 1985.

[16]     T. S. Hall, "ORBIT MANEUVER FOR RESPONSIVE COVERAGE USING ELECTRIC PROPULSION," Air Force Institute of Technology, Ohio, 2010.

[17]     C.-T. Wang, *Free Molecular Flow Over a Rotating Sphere,* Lafayette: AIAA, 1972.

[18]     A. Volkov, "Aerodynamic coefficients of a Spinning Sphere in a Rarefied-Gas Flow," *Izvestiya Rossiiskoi Akademii Nauk,* vol. 44, no. 1, pp. 167-187, 2009.

[19]     S. I. Rubinow and J. B. Keller, "The Transverse Force on a Spinning Sphere Moving in a Viscous Fluid," *Journal of Fluid Mechanics* , vol. 11, no. 3, p. 12, 1961.

American Institute of Aeronautics and Astronautics

[20]     A.-A. L. C. Cojuangco, "Orbital Lifetime Analysis of PICO- and NANO-satellites," University of Florida, Gainesville , 2007.

[21]     J. R. Wertz and W. J. Larson, SMAD, El Segundo : Microcosm Press, 2003.

[22]     V. Chobotov, Orbital Mechanics Second Edition, Reston, Virginia : American Institutre of Aeronautics and Astronautics , 1996.

[23]     P. Gurfil, Modern Astrodynamics, Butterworth-Heinemann, 2006.

[24]     AGI,          "STK          11.0.1          Programming          Interface,"          AGI,          [Online].          Available: http://help.agi.com/stkdevkit/index.html?page=source%2FSTKPlugins%2FenginePlugins_engineExtensibility.htm.

[25]     J. Wertz, Spacecraft Attitude Determination and Control, Massachusetts: D. Reidel Publishing Company, 2002.

[26]     S. Roy, R. Raju, H. F. Chuang, B. A. Cruden and M. Meyyappan, "Modeling gas flow through microchannels and nanopores," *Journal of Applied Physics,* vol. 93, no. 8, p. 10, 2003.

[27]     C.-T. Want, "Free Molecular Flow Over a Rotating Sphere," AIAA, 1972.

[28]     Analytical Graphics Inc., "STK Programming Interface," October 2013.

[29]     Blue Canyon Technologies , "Reaction Wheels," 2015. [Online]. Available: http://bluecanyontech.com/wp-content/uploads/2016/07/RW.pdf. [Accessed 18 August 2016].

[30]     HoneyBee Robotics Spacecraft Mechanisms Corporation , "Microsat CMG Attitude Control Array," [Online]. Available: http://www.honeybeerobotics.com/wp-content/uploads/2014/03/Honeybee-Robotics-Microsat-CMGs.pdf. [Accessed 18 August 2016].

[31]     "The Project," QB50, [Online]. Available: https://www.qb50.eu/index.php/project-description-obj. [Accessed 9 August 2016].

American Institute of Aeronautics and Astronautics